Published in final edited form as:
Cryobiology. 2008 August ; 57(1): 1–8. doi:10.1016/j.cryobiol.2008.03.002.

Cryopreservation of carotid artery segments via vitrification subject to marginal thermal conditions: Correlation of freezing visualization with functional recovery

S. Baicu[1], **M.J. Taylor**[1,2], **Z. Chen**[1], and **Y. Rabin**[2]

[1]Cell and Tissue Systems. 2231 Technical Parkway, N. Charleston, SC 29406

[2]Department of Mechanical Engineering, Carnegie Mellon University, Pittsburgh, PA 15213

Abstract

Cryopreservation is a well established technique for long-term storage of viable cells and tissues. However, in recent years, application of established cryobiological principles to the preservation of multicellular tissues and organs has demanded considerable attention to ways of circumventing the deleterious effects of ice and thermal stresses in bulky tissues. As part of a multidisciplinary research program designed to study the interactions of thermophysical events with tissue preservation, we report here on the implementation of a slow cooling (3°C/min) and slow warming (62°C/min) regimen towards scale-up of vitreous preservation of large tissue samples. Specifically, the correlation of thermophysical events during vitrification of carotid artery segments with function recovery is reported using marginal thermal conditions for achieving vitrification in bulky samples. Moreover, the outcome is compared with a similar study reported previously using a 3-fold higher rate of re-warming (186±13 °C/min). Tissue vitrification using an 8.4M cryoprotectant cocktail solution (VS55) was achieved in 1ml samples by imposing a low (2.6±0.1°C/min) cooling rate, between −40°C and −100°C, and a low rewarming rate (62±4°C/min) between −100°C and −40°C. Following cryoprotectant removal, the artery segments were cut into 3–4mm rings for function testing on a contractility apparatus by measuring isometric responses to four agonist and antagonists (norepinephrine, phenylepinephrine, calcium ionophore and sodium nitroprusside). In addition, non-specific metabolic function of the vessel rings was determined using the REDOX indicator alamarBlue. Contractile function, normalized to untreated control samples, in response to the agonists norepinephrine and phenylepinephrine was significantly better in the slowly re-warmed group of carotid segments (74±9% and 62±11% respectively) than for the more rapidly warmed group 31±7% and 45±15% respectively). However, EC50 sensitivities were not significantly different between the groups. Thermophysical events such as ice formation and fractures were monitored throughout the cooling and warming phases using cryomacroscopy with the aid of a purpose-built borescope device. This technique allowed a direct observation of the visual impact of ice formation on specific zones along the blood vessel segment where, in most cases, no ice formation or fractures were observed in the vicinity of the artery segments. However, in specific instances when some ice crystallization was observed to impact the artery segment, the subsequent testing of function revealed a total loss of contractility. The successful vitrification of blood vessel segments using marginal conditions of slow cooling and rewarming, provide essential information for the development of scale-up

Corresponding Author: Michael J. Taylor, Ph.D, Cell & Tissue Systems, 2231 Technical Parkway, Suite A., N. Charleston. SC 29406, mtaylor@organ-recovery.com, Tel: 843-722-6756 x17, Fax: 843-722-6657.

protocols that is necessary when clinically-relevant size samples need to be cryopreserved in an essentially ice-free state. This information can further be integrated into computer simulations of heat transfer and thermo-mechanical stress, where the slowest cooling rate anywhere in the simulated domain must exceed the critical values identified in the current study.

Keywords

Vitrification; functional recovery; blood vessels; cryomacroscopy; thermophysical events

Introduction

Extrapolation of the successful techniques for cryopreservation of cell suspensions to multicellular tissues with a defined architecture has proven to be a challenging task due principally to the damaging effects of ice formation and development of thermo-mechanical stresses, as reviewed recently by Taylor and co-workers [3;14]. In a series of studies on clinically-relevant model systems, such as a blood vessel and an articular cartilage, a markedly improved cryopreservation outcome was demonstrated were the system is preserved in an essentially ice-free state [5;7;8;14;16]. Having shown feasibility in small model systems for vitreous cryopreservation of complex tissues, the research is now aimed at scale-up experiments towards a clinically-significant sample size. This line of research relies upon a recently presented study, designed to vitrify carotid artery segments using as slow as possible cooling rates to suppress ice formation [1]. This previous study included rapid rewarming, where the rewarming rate was not a studied parameter [1]. The current study complements the recently published report by exploring the minimum rewarming rates to ensure vitrification. The current study does not merely address critical rewarming rates of the cryoprotective agent, nor the functional recovery post cryopreservation as an end result test, but the correlation between the two different effects of the process. By means of visualization, thermophysical events of crystallization, and possibly fracturing, are correlated with the quality of the recovered specimen. Promoting vitrification while preventing structural damage represent competing needs whereas there are both minimum cooling and rewarming rates to ensure vitrification, and maximum cooling and rewarming rate to avoid structural damage. Developing the knowledge about the possible balance between these competing needs serves as a prelude for attempting vitreous cryopreservation of bulky samples.

In order to explore the reasonable boundaries of cryopreservation via vitrification, a prototype imaging device, termed a “cryomacroscope”, was recently developed [4;12] to observe possible crystallization events and fracture formation in vials *in situ*, during routine cryopreservation protocols on realistic sample sizes. The cryomacroscope is applied in the current study to identify crystallization sites and fracturing during vitrification.

Experimental Methods

Carotid arteries were obtained from anesthetized New Zealand White rabbits (3.5kg male, Myrtle’s Rabbitry Inc, Thompson Station, TN) using a standard ‘no-touch’ technique as previously described [7;15]. Following excision, the blood vessel was immediately immersed in cold Dulbecco’s Modified Eagle’s Medium (DMEM) and placed on ice for transportation to the research laboratory and overnight hypothermic storage (2–6°C) as previously described [1]. In preparation for vitrification, the vessels were cleaned of extraneous tissue and cut into 2.5cm-long segments. The tissue was then loaded with cryoprotectant using a stepwise addition protocol at 0°C as shown in Fig. 1. The final concentration of the VS55 cryoprotectant mixture was 8.4M (3.1M DMSO, 2.2M 1,2-

propanediol, and 3.1M formamide). An 18G Cathlon IV catheter (32mm L × 1.32mm ID) was carefully inserted into the vessel and tied in place to allow the loading of the cryoprotectant by gravity driven perfusion, while the vessel--with the attached cannula--was immersed in cold VS55 of the appropriate concentration for stepwise addition of the VS55 cocktail. Following cryoprotectant loading, the catheter was removed while the suture was left in place and the tissue was immersed in 1mL of pre-cooled VS55 in a 20 mL glass scintillation vial. The sample vial was mounted on a the cryomacroscope and connected to a computer data acquisition system, to allow real time visualization and recording of the cryopreservation process, as well as the sample thermal history, as previously described [1;4]. For thermal history mentoring, a thermocouple was wired through a guiding sleeve into the vial, and immersed into the cryoprotectant, touching the center of the vial base.

Tissue vitrification was performed by imposing a low cooling rate (2–3°C/min) at the upper part of the cryogenic temperature range, between −40°C and −100°C, and a low rewarming rate (60°C/min) when passing through this temperature range again during the rewarming phase of the protocol. To achieve the cooling rate of 2–3°C/min, the sample vial was placed in a delrin sleeve, having a wall-thickness of 15mm and then pre-cooled to 0°C. Next, with the surrounding sleeve, the vial was lowered in a glass beaker of air placed in the vapor region above boiling liquid nitrogen to be cooled from −40°C to −130 °C as previously described [1][4]. After reaching −130°C, the sample vial–sleeve assembly was moved to ambient air for the first re-warming phase, in the temperature range of −130°C and −100°C (H3, Table 1). When the sample temperature reached −100 °C, the thick sleeve used during cooling was replaced with a thin-wall sleeve, having a thickness of 3mm, initially at room temperature; the new sleeve-vial assembly was left in the ambient air until the temperature reached −40°C (H4, Table 1). The vessel was then transferred to a ‘fresh’ sample of VS55, the suture was removed, the catheter was reattached, and the cryoprotectant unloading process was started following the steps shown in Fig. 1. The technique described above was devised to achieve the desired temperature rates and to ensure that the heat transfer conditions and sleeve replacement technique were rapidly performed without interrupting the normal course of temperature dynamics and cryopreservation process.

Following cryoprotectant removal, the vitrified segments were cut into 3–4mm long rings. For contractility testing each ring, either vitrified or untreated control rings from the same artery, was mounted between two stainless-steel wire hooks, suspended in a physiological temperature tissue organ bath (Radnoti Glass Technology, Monrovia, CA) containing 5 mL of continuously gassed (95%O2–5%CO2) Krebs-Henseleit (KH) solution. After one hour of equilibration, the baseline pre-tension of each artery ring was adjusted to 1g-force and the isometric response to a selection of four agonist and antagonists (norepinephrine (NP), phenylepinephrine (PP), calcium ionophore (Ca-I), and sodium-nitroprusside (SNP) was employed to assess the endothelium-independent and dependent smooth muscle cell mechanical function. Changes in ring tension relative to baseline, in response to various doses of these pharmaceutical agents, were recorded by a digital data acquisition and analysis system (Gould Instruments Systems, Valley View, OH). Following exposure to NP (6 doses), the rings were washed for one hour with KH buffer to remove the agonist and to bring the rings to their initial baseline tension. Then, the rings were consecutively exposed to PP (6 doses), Ca-I (2 doses, endothelium-dependent smooth muscle relaxation), and SNP (2 doses, endothelium-independent smooth muscle relaxation) without intermediate washing and tension adjustments. Each ring’s maximal response (contraction or relaxation) to each dose of the above mentioned pharmaceutical agents was recorded after subtracting the appropriate baseline.

The metabolic activity of cryopreserved and fresh control rings was determined using a non-invasive non-specific cell indicator, alamarBlue (Trek Diagnostics Systems, Cleveland,

OH). This test incorporates a water-soluble oxidation-reduction (REDOX) indicator that fluoresces and changes color in response to innate cellular metabolic activity. After 3 hours of ring's incubation (37 °C, 5% CO_2) with 10% alamarBlue working solution, 100 μL aliquots of the supernatant medium were placed in a 96-well plate and read on a microtiter plate spectrofluorometer at 590 nm. The relative fluorescence intensity was normalized to the dry weight of the tissue and expressed in percent normalized fluorescence intensity of untreated controls.

Results and Discussion

The current study is an important part of an ongoing research program that seeks to examine and document thermo-physically and, by subsequent viability testing, the ice-free cryopreservation of clinically relevant large-size tissue samples. The latter requires scaling up of cryoprotectant volume while optimizing cooling and warming heat transfer rates, to avoid crystallization and to reduce thermo-mechanical stress, in order to prevent fracture formation. This phased approach, which integrates the study of thermophysical properties with cryobiology, is intended to both increase our knowledge of vitrification of tissues and to provide the basis for an enabling technology for improved cryopreservation of both native tissues and engineered tissues, to be used in the burgeoning fields of tissue engineering and regenerative medicine.

In a previous study [1], the feasibility of vitrification of blood vessel segments was demonstrated both visually and by mechanical viability testing. Pre-established optimum cooling and heating protocols [1;12] were employed for the ice-free cryopreservation of either rings or segments of carotid arteries in 1 mL of VS55. Irrespective of tissue sample size (rings or segments), real time recorded cryomacroscope images showed successful vitrification free of macroscopic crystallization and fractures subject to slow cooling (2–3°C/min). The absence of devitrification or re-crystallization at high rewarming rates (190°C/min) was further demonstrated there. Moreover, these thermal conditions maintained tissue mechanical contractile and relaxation function and preserved tissue metabolic activity when the sample size was increased from 3–4mm-long rings to 2.5cm-long artery segments [1]. For the vitrification process, the latter--modeled on rabbit carotid artery--represented the next necessary validation step in tissue sample scale-up from rings. The ice-free cryopreservation of large size tissue samples usually requires large volumes of cryoprotectant (1mL<) and therefore corresponding optimized low cooling/low rewarming rates that will help reduce and/or avoid thermo-mechanical stress. Thus, as an extension of the prior studies, the current study evaluated the effects of vitrification on tissue function and viability of 2.5cm long carotid artery segments using a combination of slower rates of heat transfer. More specifically, the low cooling rate used previously during segment vitrification in 1mL of VS55 cryoprotectant, was now coupled with a modified rewarming regimen employing a low heat transfer rate in preparation for cryoprotectant volume up-scaling.

In the present study low cooling (2–3°C/min from −40°C to −100°C) and low rewarming (60°C/min, between −100°C and −40°C) rates were imposed. As mentioned, the former has been validated as an optimum ice-free cryopreservation cooling rate for the present animal model, while coupled with a fast rewarming rate of 186±13°C in the same temperature range [1] (see Table 1 for a complete list of cooling and rewarming rates). For both fast and slow warming conditions, at −130 °C the vial–sleeve assembly was moved to ambient air for the first re-warming phase (H3). At −100 °C, two different thermal conditions/heat transfer media were employed for the second warming phase (H4): a room temperature 3mm-wall thickness sleeve in ambient air and, a room temperature 30%DMSO-water bath, respectively.

Recovery of tissue function

The isometric percent maximal contractile response was plotted versus the negative logarithm (base10) of the agonist dose and presented as dose/response curves in Fig. 2. For comparative purposes the results obtained using the low cooling rate with two different second phase warming rates (H4) were included. Artery segment vitrification at low re-warming rate better preserved the smooth muscle cells contractile function when compared to fast re-warming. The difference was statistically significant ($P<0.01$) for the norepinephrine two highest doses. Relative to untreated controls the cryopreservation process significantly reduced vessel maximal contractile response, irrespective of warming rates, Table 2. However, the response of vitrified samples to the agonist used was influenced by the heat transfer rates, low rate re-warming doubled the contractility of arterial segments stimulated with norepinephrine. Although not statistically significant, phenylepinephrine induced smooth muscle contractility was better preserved using slow warming. It has to be mentioned that rings exposure to PP succeeded one hour (4 of 15 min intervals) of 37 °C washing/equilibration in KH that, in turn, followed tissue contraction in the presence of six incremental doses of NP. Generally, the extensive washing in KH could not completely remove and/or relax the tissue to the baseline tension. Prolonging the washing to two hours did not improve the situation. The EC50 value, the concentration for the half-maximal response for each agonist was calculated by logistic analysis and was conventionally expressed as sensitivity $pD2=-LOG_{10}[EC50]$, Table 3. The vitrified vessels sensitivity to the two agonists used was slightly reduced in comparison to fresh control tissue, yet not statistically significant. The two rewarming conditions had no influence on vessels sensitivity.

Smooth muscle relaxation testing showed that slowly rewarmed vitrified samples produced significantly ($P<0.05$) less maximum endothelium-dependent relaxation of the precontraction in the presence of Ca-I antagonist (Table 4). Endothelium-independent smooth muscle contraction was maintained in vitrified samples relative to fresh tissue and was not influenced by the warming heat transfer rates. Tissue metabolic activity was somewhat reduced after vitrification and was not changed by the rewarming rates used (Table 4).

Visualization of thermo-physical events and correlation with tissue function

Some ice nucleation/crystallization was visualized during cooling in most of the experiments. In general, the sites of nucleation were very few (1 to 3 locations only) and conditions were such that ice crystal growth was highly attenuated. These observations are consistent with the notion that these conditions of cooling are marginal for achieving complete vitrification of the VS55 cryoprotectant cocktail. Extraneous materials in the system such as the suture and the thermocouple provided consistent nucleation sites, but the positioning of other sites of ice formation on the artery segment surface was random with one to three locations on average, and total ice area coverage was minor relative to vessel length. The cryomacrographs of a typical arterial segment vitrification are presented in Fig. 3. Crystallization in this case is localized near the middle of the vessel (panel B and panel C; see panel D for assistance in identification), which was directly correlated with tissue viability at the same locations; the ring cuts from the segment where sequentially numbered in the process of preparation for testing. Overall, mechanical function of the vessel was preserved, where a high vessel contractile response of 80.72% and 79.27% for NP and PP, was recorded relative to the fresh rings, respectively. In contrast, the ring sectioned post-vitrification from the middle ice covered region performed poorly (ring#6, Table 5). All the other rings were recovered from the ice-free region of the artery following removal of the previously cannulated section of the vessel (Fig. 3(C, D)). This particular ring (#6) had a weak response when stimulated with endothelium-independent antagonist, yet had fresh-

comparable relaxation in the presence of Ca-I, the endothelium-dependent smooth muscle antagonist (Table 5).

Based on recorded images, a correlation can be seen between the formation of ice crystals and tissue contractile function. As a general trend, rings cut from vitrified segments at the vicinity ice crystallization sites had none or very little response to the pharmaceutical agents used. The response was directly related to the extent of ice formation and its depth of penetration into the artery wall. Two ice crystallization sites were consistently observed during cooling of different specimens: 1) at the tip of the temperature probe, and 2) at the blood vessel cannulation-suture site. For the former site, area coverage by ice formation was localized and confined to the vicinity of the temperature probe (see Figs. 3 & 4). The cryoprotectant between the probe and the vessel appeared completely vitrified, with a clean transparent appearance. Ice formation confined to this area did not appear to impact the blood vessel segment and had no effect on tissue viability and functionality.

The second consistent nucleation site—in the area of the suture left around the vessel after removal of the post-cryoprotectant loading and prior to sample vitrification—had a significant impact on the cryopreservation outcome. However, leaving the suture in place was deemed critical for the success of this study from the reason described hereon. The last cryoprotectant loading step (Fig. 1) involved the highest VS55 concentration and needed to be concluded on the cryomacroscope setup in order to avoid prolonged tissue exposure to the potentially toxic environment at elevated temperatures. It has proven necessary to remove the cannula rapidly, while leaving the suture in place, for sample transfer to the glass vial prior to vitrification. After rewarming the sample and prior to sectioning the artery segment into rings for contractility testing, the vessel extremity inclusive of the suture up to the cannula tip location within the artery was removed and discarded. This was necessary because cannula advancement into the lumen and the mechanical tension induced by suture fastening around the artery can destroy endothelial integrity and diminish vessel mechanical properties. Irrespective of location and size, the thawing process of all cooling-phase ice formations was initiated immediately at the beginning of second warming phase, at −100°C.

With the aid of the cryomacroscope, ice formation and growth on the vessel surface could be clearly observed and recorded. However, no visual information could be provided about the depth of the ice layer within the vessel wall. The latter is anticipated to have greatly impacted vessel viability and function, triggering variable results.

Further in-depth observations during this study were provided by two aberrant experiments which did not conform to the planned regimen of cooling and warming. Nevertheless, the deviant conditions provided useful and informative observations derived from the cryomacroscope images. Both had a similar cryopreservation visual outcome, yet tissue viability based on subsequent mechanical and metabolic testing was significantly different. Those two experiments were excluded from the experimental group and were not part of the statistical analysis. Nevertheless, they validate the role of the cryomacroscope in documenting the vitrification process and providing information on the approaches for scaled-up ice-free cryopreservation. It is assumed that accidental prolonged exposure of the sample vial to ambient high humidity levels, and improper cleaning and moisture removal of the temperature probe guiding sleeve could explain the events observed in these two experiments as described below.

The first experiment is considered as a “negative control” due to the fact that no detectable mechanical function was observed post vitrification, while the metabolic activity was extremely low, at a level of 7.9% of the corresponding control tissues (the group average was 80.9% (N=8)). In this case, cooling-phase ice crystallization was initiated below −50°C

and reached full macroscopic development with ice covering the entire surface of the artery segment before the temperature of −100°C was reached (Fig. 5). The ice spread started from the edge toward the center of the vial, around the vessel, and from the suture site. No crystallization was visible around the temperature probe in this particular case (Fig. 5). Moreover, fracture formations were seen in the glassy vitrified region of VS55 at −130°C, on the lower left vial circumference and on the vial side opposite to the location of the vessel segment. The fractures fused and became unidentifiable above −130°C, during the first rewarming phase. Subsequently, ice formations began thawing following sleeve replacement at −100°C. Unique to this experiment, the two rates of cooling were H1=1.53°C/min and H2=0.74°C/min, which were considerably lower in comparison with the corresponding group average rates (2.58°C/min and 1.44°C/min, respectively, Table 1). This, in part, justified their exclusion from the group analysis as outliers for the reasons explained above. Nevertheless, in another sense they were fortuitous events that provided useful observations relevant to interpretation of these experiments. Analyses of thermo-mechanical stress development in cases of partial crystallization [9], high cooling rates [11], and a similar vial setup but with a different cryoprotectant [10]have been presented by Steif and co-workers, as a part of the current research program.

Results of the second aberrant experiment are displayed in Fig. 4. Ice formed initially at the vessel edge and grew toward the center of the vial and around the suture. It continued to grow as temperature decreased (Fig. 4(C)) until the next target demarcation in the direction of vial center was reached. At −80°C ice crystallization was initiated around the temperature probe yet it remained confined to the close proximity of the probe and did not impact the artery segment (Fig. 4(C)). As in the previous experiment, cooling-phase ice formations began thawing subsequent to sleeve replacement at −100°C (Fig. 4(D)) during re-warming. No fractures were observed in this experiment and all heat transfer rates were aligned with the reported group average values (Table 1).

In contrast to the negative control results displayed in Fig. 5, a mechanical response to the two agonists used was observed in the experiment referred to in Fig. 4, yet inconsistent and weak. Comparing ice coverage in Fig. 4(D) with Fig. 5(C), the amount of ice is consistent with worst recovery results obtained from the negative control experiment. For the experiment shown in Fig. 5 a vessel average maximum contractile response of 18.0% for NP and 12.6% for PP was obtained relative to the corresponding fresh unpreserved tissue, while the analogous group (N=8) average values were 73.7% and 62.3%, respectively. The metabolic activity was quantified as 67.8% of the corresponding fresh control (80.9% (N=8) for the group average).

The observations in these experiments, showing that some ice formation within the system can be tolerated without negatively impacting tissue structure and function, is consistent with some much earlier work using an entirely different system. Using freeze substitution techniques it has been shown that the location and distribution of ice in smooth muscle tissue is influenced by cooling rate and that this, in turn, had a marked influence on contractile recovery [2;13;14]. As we have reviewed recently, the unequivocal conclusion from studies of that type was that the amount and location of extracellular ice has a dramatic effect on the post-thaw function of complex tissues and organs. As a result, it is generally thought that cryopreservation of multicellular tissues and organs will mandate that the amount of ice in the system is limited, restricted to harmless sites, or ideally, that ice crystallization is prevented altogether[14].

Summary

The results of this study confirmed that ice-free cryopreservation of 2.5cm-long carotid artery segments is feasible using 1mL of VS55 and relatively low cooling and warming rates. These conditions sustain contractile function and metabolic activity to a high degree. Moreover, they help avoiding fracture formation during cooling and devitrification and/or re-crystallization during rewarming. Visualization by the cryomacroscope was found essential for such verification. Moreover, based on the cryomacroscope recording, the extent of ice growth location and volume on the vessel could be identified during the vitrification process. Therefore, future clinical complications associated with transplantation could be reduced based on the actual history of the vessel. The successful vitrification of blood vessel segments at low cooling rates, followed by slow rewarming rate, provide essential information for the development of scale-up protocols that is necessary when clinically-relevant size samples need to be cryopreserved in an essentially ice-free state. This information can further be integrated into computer simulations of heat transfer and thermo-mechanical stress, where the slowest cooling rate anywhere in the simulated domain must exceed the critical values identified in the current study.

Acknowledgments

We are grateful to Elizabeth Greene for her meticulous care in harvesting the arteries for these studies.

This study was supported by NIH/NHLBI grant # RO1HL06994401A1,02,03,04

References

1. Baicu S, Taylor MJ, Chen Z, Rabin Y. Vitrification of Carotid Artery Segments: An Integrated Study of Thermophysical Events and Functional Recovery Towards Scale-up for Clinical Applications. Cell Preservation Technology. 2007; 4(4):236–244. [PubMed: 18185850]
2. Hunt CJ, Taylor MJ, Pegg DE. Freeze-substitution and isothermal freeze fixation studies to elucidate the pattern of ice formation on smooth muscle at 252K (−21 C). J Microsc. 1982; 125(2): 177–186. [PubMed: 7086882]
3. Rabin, Y.; Steif, PS. Solid Mechanics Aspects of Cryobiology. In: Baust, JG.; Baust, JM., editors. Advances in Biopreservation. Boca Raton; CRC Press: 2006. p. 353-375.
4. Rabin Y, Taylor MJ, Walsh JR, Baicu S, Steif PS. Cryomacroscopy of vitrification, Part I: A prototype and experimental observations on the cocktails VS55 and DP6. Cell Preserv Technol. 2005; 3(3):169–183. [PubMed: 16721425]
5. Song YC, An YH, Kang QK, Li C, Boggs JM, Chen Z, Taylor MJ, Brockbank KGM. Vitreous Preservation of Articular Cartilage Grafts. Journal of Investigative Surgery. 2004; 17:1–6. [PubMed: 14761821]
6. Song YC, Hagen PO, Lightfoot FG, Taylor MJ, Smith AC, Brockbank KGM. In vivo evaluation of the effects of a new ice-free cryopreservation process on autologous vascular grafts. Journal of Investigative Surgery. 2000; 13(5):279–288. [PubMed: 11071564]
7. Song YC, Khirabadi BS, Lightfoot FG, Brockbank KGM, Taylor MJ. Vitreous cryopreservation maintains the function of vascular grafts. Nature Biotechnology. 2000; 18:296–299.
8. Song YC, Lightfoot FG, Chen Z, Taylor MJ, Brockbank KGM. Vitreous Preservation of Rabbit Articular Cartilage. Cell Preservation Technology. 2004; 2(1):67–74.
9. Steif PS, Palastro M, Rabin Y. Analysis of the effect of partial vitrification on stress development in cryopreserved blood vessels. Medical Engineering & Physics. 2006; 29(6):661–670. [PubMed: 16996295]
10. Steif PS, Palastro M, Rabin Y. Continuum mechanics analysis of fracture progression in the vitrified cryoprotective agent DP6. ASME J Biomech Eng. In press.

11. Steif PS, Palastro M, Rabin Y. The effect of temperature gradients on stress development during cryopreservation via vitrification. Cell Preservation Technology. 2007; 5(2):104–115. [PubMed: 18185851]

12. Steif PS, Palastro M, Wan CR, Baicu S, Taylor MJ, Rabin Y. Cryomacroscopy of vitrification, Part II: Experimental observations and analysis of fracture formation in vitrified VS55 and DP6. Cell Preserv Technol. 2005; 3(3):184–200. [PubMed: 16900261]

13. Taylor MJ, Pegg DE. The effect of ice formation on the function of smooth muscle tissue following storage at −21 C and −60 C. Cryobiology. 1983; 20:36–40. [PubMed: 6831909]

14. Taylor, MJ.; Song, YC.; Brockbank, KGM. Vitrification in Tissue Preservation: New Developments. In: Benson, E.; Fuller, BJ.; Lane, N., editors. Life in the Frozen State. London: CRC Press; 2004. p. 603-641.

15. Taylor MJ, Song YC, Chen ZZ, Lee FS, Brockbank KG. Interactive Determinants for Optimized Stabilization of Autologous Vascular Grafts during Surgery. Cell Preservation Technology. 2004; 2(3):198–208.

16. Taylor MJ, Song YC, Khirabadi BS, Lightfoot FG, Brockbank KGM. Vitrification fulfills its promise as an approach to reducing freeze-induced injury in a multicellular tissue. Advances in Heat and Mass Transfer in Biotechnology. 1999; 44:93–102.

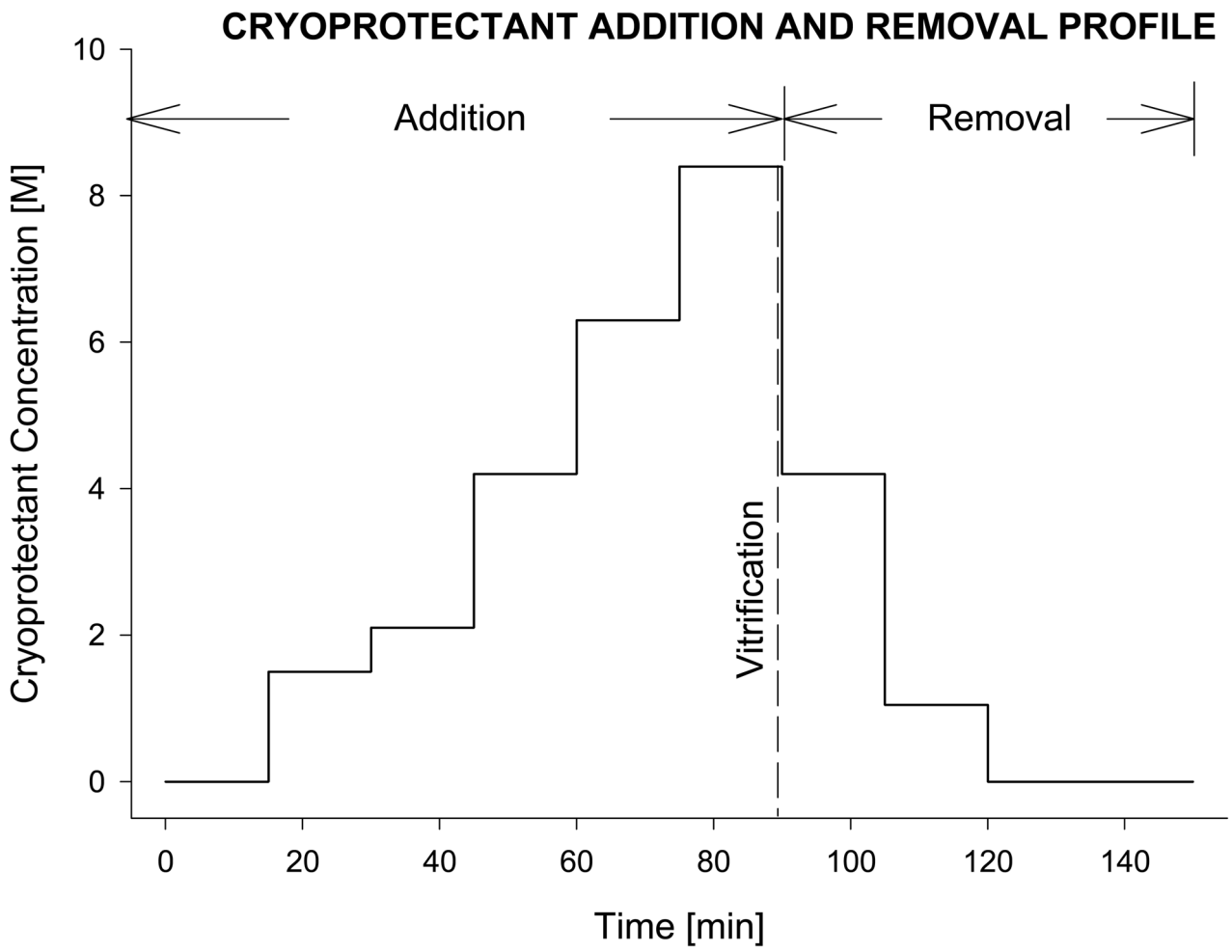

Figure 1.

Schematic diagram of the sequential incubation steps, adapted from a previously reported technique for adding and removing the vitrification cocktail, VS55 [16]. For vessel segments, the process was facilitated by gravity perfusion of the solutions through the lumen of the artery segment [6]. Similarly, after vitrification and rewarming, the tissue samples were returned to physiological medium by eluting the cryoprotectants sequentially, using stepped changes. The cryoprotectant solution used at each step in the dilution was supplemented with 300mM mannitol as an osmotic buffer, to prevent excess cell swelling.

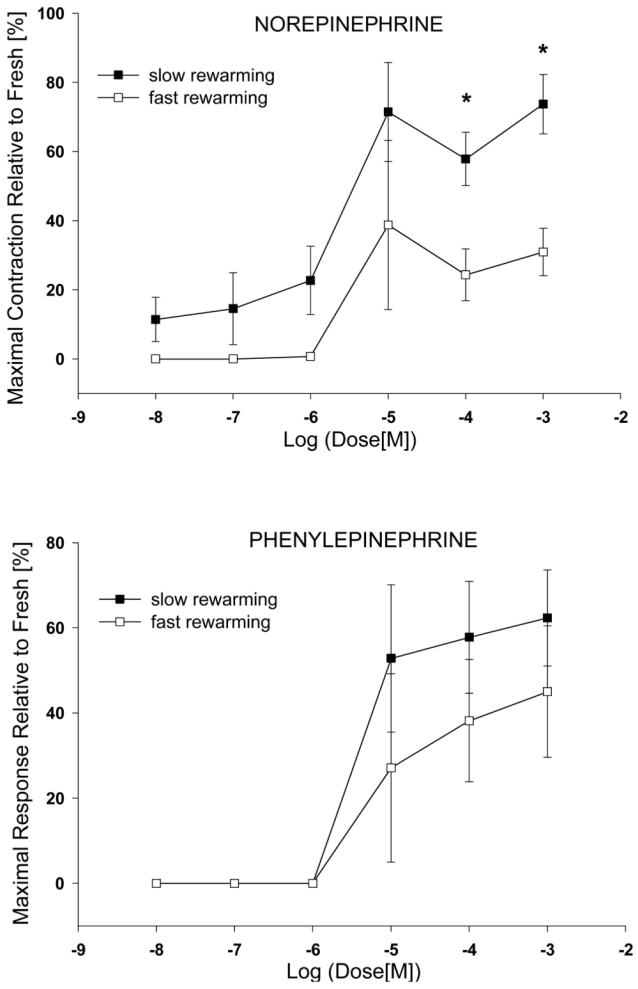

Figure 2.
Contractile dose-response curves to norepinephrine and phenylepinephrine for vitrified arterial segments. The values are expressed as mean±sem percentage of maximal force generated relative of the fresh control.

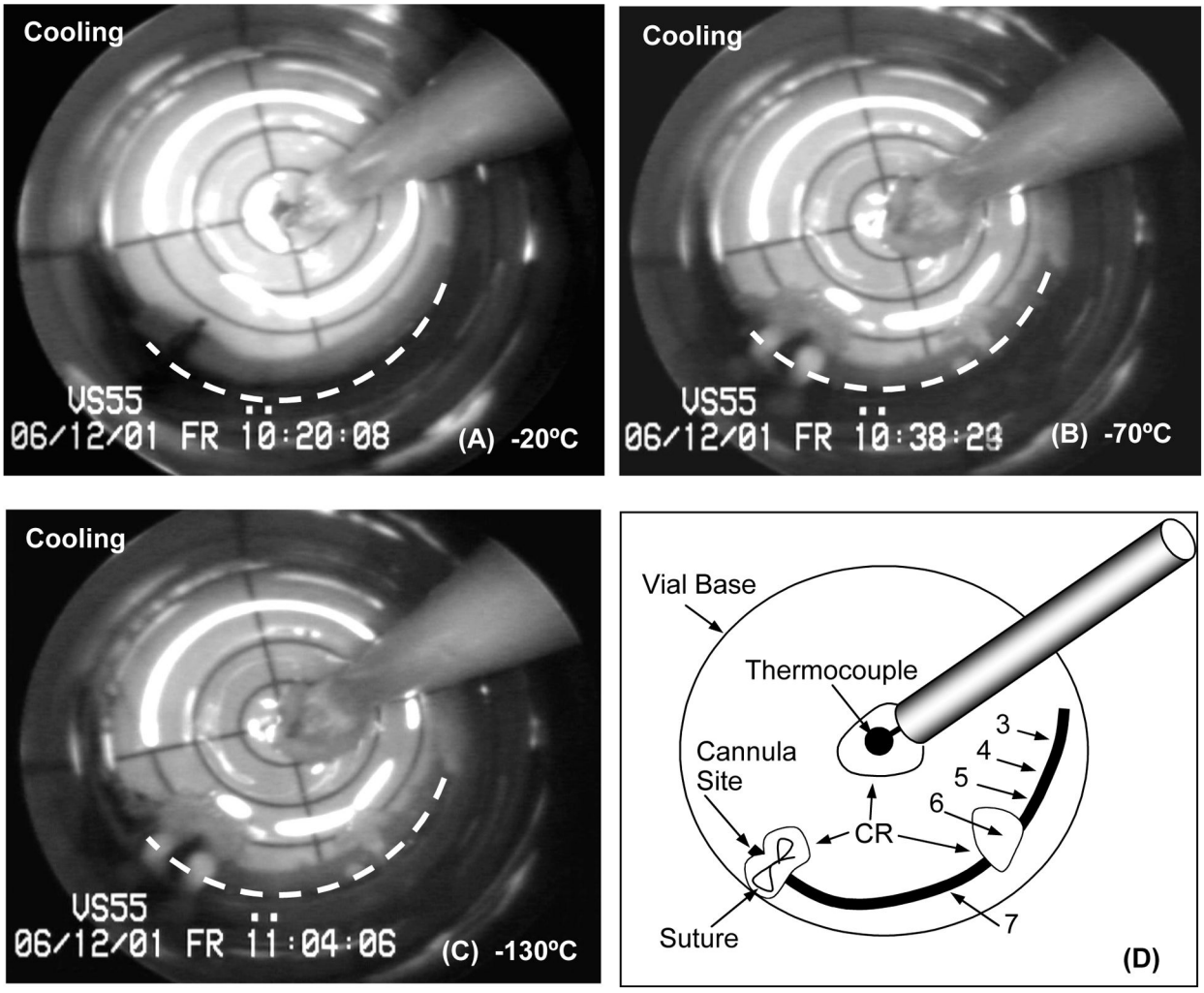

Figure 3.

Representative cryomacrographs of a 25mm-long carotid artery segment vitrification using low cooling and warming rates. The vessel centerline is represented by a dashed white line. Panel (D) shows a schematic diagram of the cryomacrograph in (C). In Panel (D) rings tested for mechanical function post-vitrification are labeled from 3 to 7 starting at the artery free-end. Rings #1 and #2 were cut prior to vitrification and served as fresh-control rings during mechanical testing. Vessel extremity inclusive of the suture up to the site of the original cannula tip location within the artery was removed prior to ring sectioning (Panel D). The location of ice crystallization (CR) in relation to the assignment of rings for subsequent testing is indicated on the Panel (D) schematic.

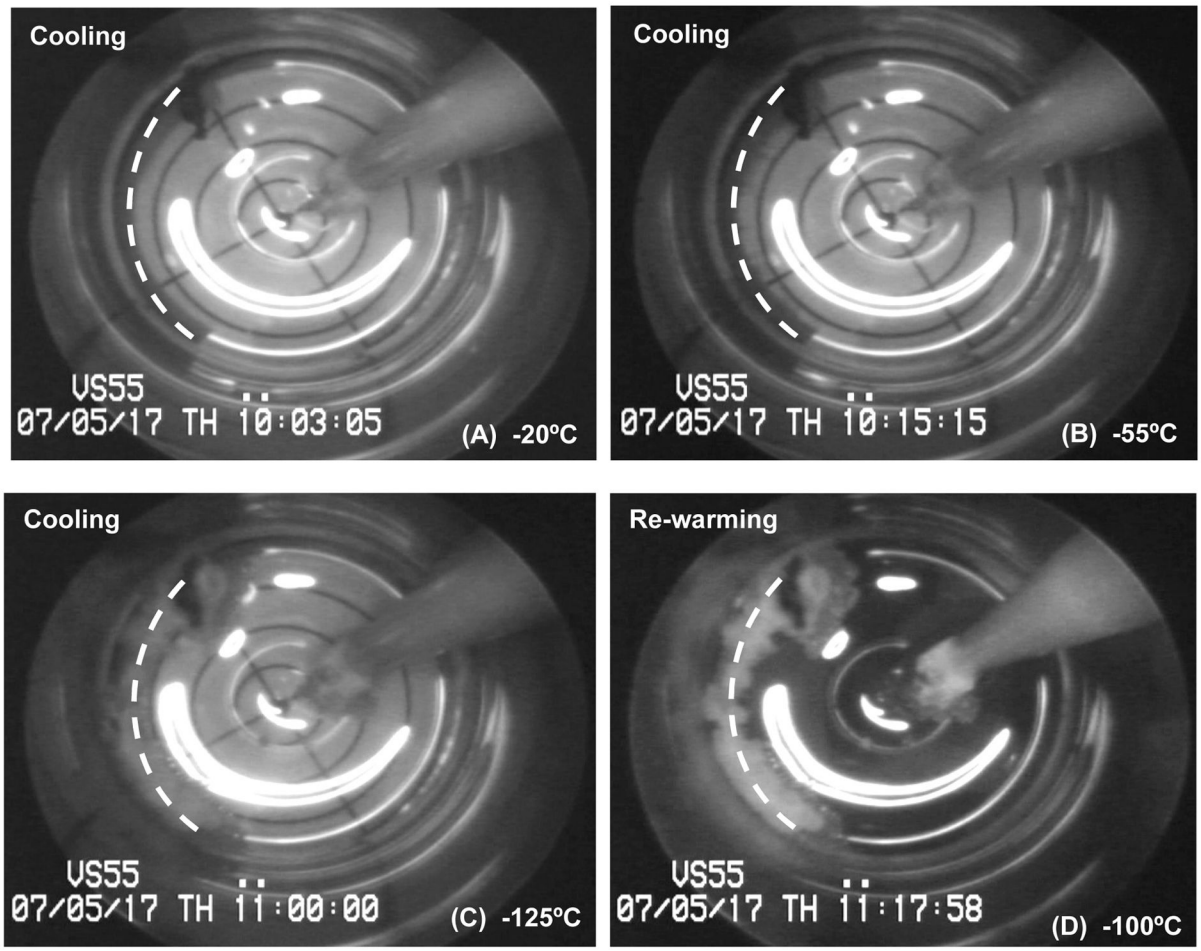

Figure 4.

Cryomacrographs of ice formation during slow cooling vitrification of a vessel segment. The vessel centerline is represented by a dashed white line. Following vitrification, low contractility was observed in the presence of both NP and PP, while a fresh comparable metabolic activity was measured. Nucleation and ice-crystallization around the vessel started below −50°C, Panel (B). Ice crystallization was initiated around the temperature probe at −80°C, yet it remained confined to probe vicinity, Panel (C). Panel (D) image was taken at −100°C during rewarming, right at the moment of sleeve replacement. No fractures were visible in this experiment.

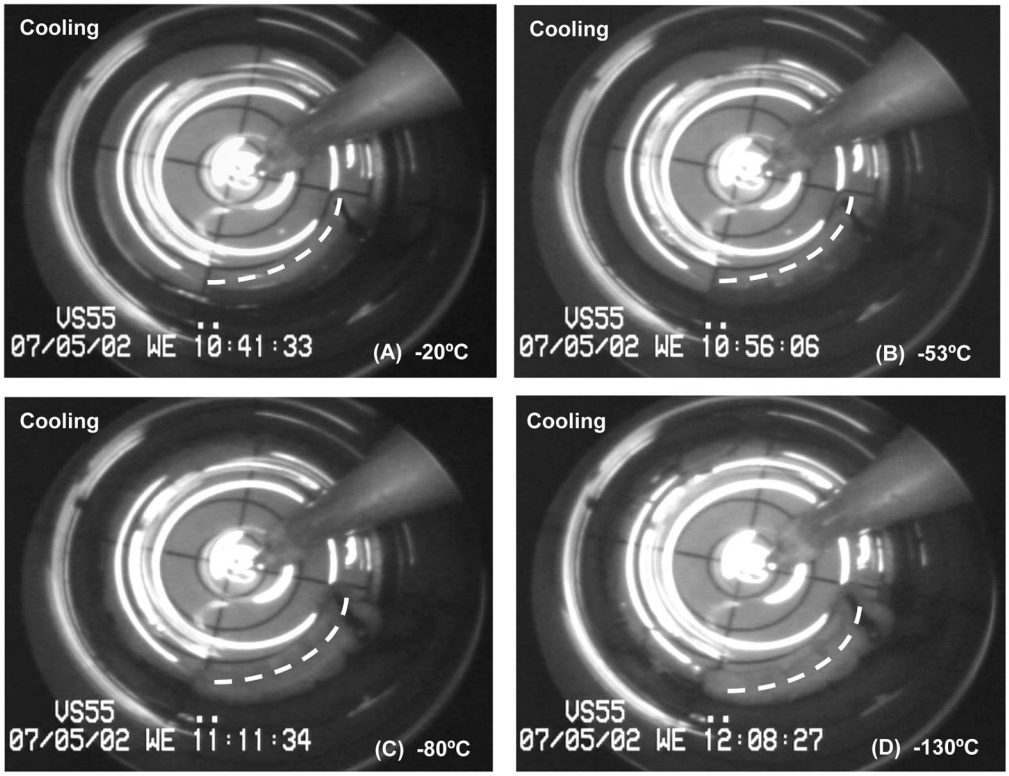

Figure 5.
Cryomacrographs of so-called “negative control” vitrification. The vessel centerline is represented by a dashed white line. Viability testing detected no mechanical function and extremely low metabolic activity post slow cooling/slow rewarming cryopreservation. Fractures were seen (Panel D) on the tissue opposite side of the vial and on the lower left side of the vial, near the suture end of the vessel segment.

Table 1

Cooling and rewarming rates applied in the current study and in a previous study [1]

Heat Transfer Rates	Slow Cooling Slow Re-warming (N=8)	Slow Cooling Fast Re-warming (N=7)[1]
H1 (−40°C to −100°C)	2.58±0.11	2.54±0.15
H2 (−100°C to −130°C)	1.44±0.09	1.34±0.13
H3 (−130°C to −100°C)	5.31±0.14*	4.71±0.18
H4 (−100°C to −40°C)	61.9±4.01#	186±13.3

Data are expressed in °C/min and presented as mean ± sem.

*P=0.0541, compared to fast re-warming conditions;

#P<0.001, compared to fast re-warming conditions.

Table 2

Maximal contractile response of vitrified carotid artery

	Slow Cooling/Slow Rewarming (N=8)			Slow Cooling/Fast Rewarming (N=7)		
	Vitrified(g)	**Fresh Control (g)**	**%**	**Vitrified(g)**	**Fresh Control (g)**	**%**
Norepinephrine	1.99±0.36 *,+	2.65±0.33	73.7±8.6 #	0.54±0.14 *	1.83±0.19	30.9±6.9
Phenylepinephrine	1.89±0.47 *	2.76±0.40	62.3±11.3	0.79±0.27 *	2.05±0.26	45.0±15.4

Data are expressed in gram (g) of maximal tension generated and are presented as mean ± sem.

*P<0.05, vitrified vs. corresponding fresh control group (Nonparametric Wilcoxon t-test);

+P<0.01 compared to fast re-warming vitrified group (Nonparametric Mann-Whitney t-test);

#P<0.01 compared to fast re-warming conditions (Nonparametric Mann-Whitney t-test).

Table 3

Carotid artery sensitivity (pD2) to contractile agonists

	Slow Cooling/Slow Re-warming (N=8)		Slow Cooling/Fast Re-warming (N=7)	
	Vitrified	**Fresh Control**	**Vitrified**	**Fresh Control**
Norepinephrine	5.53±0.14	5.88±0.1	5.37±0.13	5.94±0.22
Phenylepinephrine	5.29±0.13	5.48±0.15	5.27±0.20	5.56±0.21

Data are presented as mean ± sem.

Table 4

Viability results of vitrified carotid artery

	Slow Cooling/Slow Re-warming (N=8)	Slow Cooling/Fast Re-warming (N=7)
	% relative to fresh	% relative to fresh
Ca-I relaxation	11.0±6.9 *	77.1±35.1
SNP relaxation	162.7±37.7	125.6±57.0
alamarBlue	80.9±7.7	91.0±17.8

Data are expressed in percentage relative to fresh unpreserved group and are presented as mean ± sem;

* P<0.05 compared to fast re-warming conditions.

Table 5

Mechanical function post whole segment vitrification of representative individual rings (slow cooling, slow warming conditions)

Maximal Contractile Response	Fresh Rings		Rings from Vitrified Vessel				
	Ring#1	**Ring#2**	**Ring#3**	**Ring#4**	**Ring#5**	**Ring#6**	**Ring#7**
Norepinephrine	4.43	4.95	4.15	6.29	4.91	0.24	3.34
Phenylepinephrine	4.79	4.59	4.21	6.04	4.76	0.32	3.26
Calcium -Ionophore	−0.46	−0.04	−0.08	−0.23	−0.01	−0.14	−0.09
Sodium-Nitroprusside	−0.72	−1.48	−2.30	−4.88	−3.66	−0.12	−2.07

Data are expressed in gram (g) of maximal tension generated for the highest agonist and antagonist concentration (10^{-4} M). Rings #1 and #2 were cut prior to cryopreservation. Rings #3 through #7 were sectioned starting from the free end of the vessel toward the cannula site. Ring#6 was cut from the middleice covered section of the artery.